ChemComm

COMMUNICATION

View Article Online
View Journal | View Issue

Cite this: *Chem. Commun.*, 2022, **58**, 10532

Received 30th May 2022,
Accepted 21st June 2022

DOI: 10.1039/d2cc03052g

rsc.li/chemcomm

A pH-responsive crosslinker platform for antibody-drug conjugate (ADC) targeting delivery†

Francesca Migliorini, Elena Cini, Elena Dreassi, Federica Finetti, Giovanni Ievoli, Giulia Macrì, Elena Petricci, Enrico Rango, Lorenza Trabalzini and Maurizio Taddei *

We report a new 1–6 self-immolative, traceless crosslinker derived from the natural product gallic acid. The linker acts through a pH-dependent mechanism for drug release. This 5-(hydroxymethyl)pyrogallol orthoester derivative (HMPO) was stable for 24 hours at pH values of 7.4 and 6.6 and in plasma, releasing molecules bound to the hydroxymethyl moiety under acid-dependent stimuli at pH 5.5. The linker was non-toxic and was used for the conjugation of Doxorubicin (Doxo) or Combretastatin A4 with Cetuximab. The ADCs formed showed their pH responsivity reducing cell viability of A431 and A549 cancer cells better than Cetuximab alone.

Conjugation between a targeting moiety and a drug is one of the most efficient methods for overcoming drug selectivity problems.[1] Besides antibody-drug conjugates (ADCs),[2] there are excellent examples of conjugates containing integrin,[3] carbonic anhydrase ligands,[4] folic acid,[5] prostate specific antigen (PSA)[6] or somatostatin.[7] Conjugation allows an increase in drug concentration in the tissues where the target is located after the drug cargo has been selectively activated at the site of action. Release is controlled by a trigger mechanism that depends on the linker, the key component of the conjugation system.[8] The way the linker is removed (and the drug released) depends on the trigger mechanism. Historically, the first external stimulus used to release drugs from a ADC was pH.[9] In cancer, mechanisms related to abnormal rapid metabolism and proliferation lead to a hypoxic microenvironment in which several acidic molecules are produced that lower the pH to around 5.7–6.9.[10] Within the tumour cell, the proton influx lowers the intracellular and substructural pH to 5.0–6.0, while a lower pH (4.0–5.0) is achieved in the lysosomes.[11] The pH difference between tumour cells and healthy tissue has been exploited to produce pH-responsive anti-cancer nanomaterials,[12] although the presence of an acidic tumour microenvironment poses a potential problem for selectivity. At ADC, once the antibody reaches its target, the internalisation of the receptor selectively transports the conjugate into the interior of the cell to be eventually metabolised in the acid lysosome environment.[2a] FDA-approved acylhydrazones (found in Mylotarg® and Besponsa®), for example, release the active ingredient in acidic environments, but can only be made from carbonyl or hydrazine derivatives, limiting the delivery to agents that contain these functions.[13] The bifunctional cross-linker *N*-ethoxybenzylimidazole (NEBI) has been used as a tunable pH-sensitive linker and used for targeted delivery of indenoisoquinoline agents or modified Doxo to cancer tissue (Scheme 1).[5d,14] In this case, a benzaldehyde or an imidazole moiety remains in the released drug. Maleimido derivatives, after hydrolytic conversion to monoamides of maleic acid, have a proximal carboxylate group that supports amide hydrolysis with the formation of the malic anhydride under acidic conditions.[15] Although efficient, this linker is limited to transporting only primary amines (Scheme 1).[1]

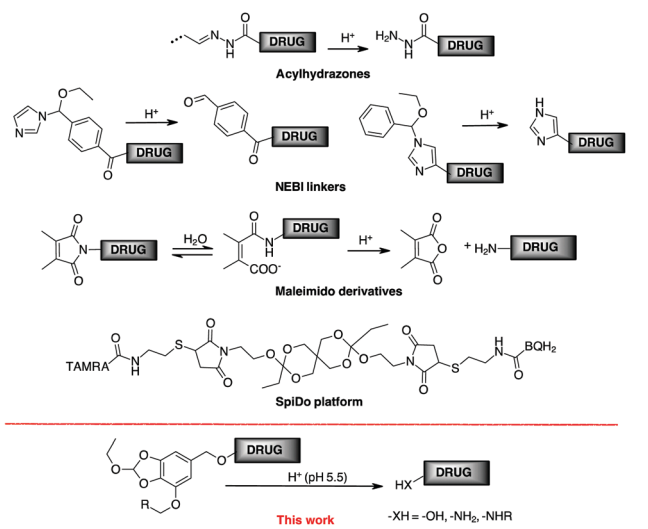

Scheme 1 Examples of acid labile linkers for drug targeting.

Dipartimento di Biotecnologie, Chimica e Farmacia, Università degli Studi di Siena, Via A.Moro 2, 53100 Siena, Italy. E-mail: maurizio.taddei@unisi.it

† Electronic supplementary information (ESI) available. See DOI: https://doi.org/10.1039/d2cc03052g

Wagner and co-workers have determined the release kinetics of several functional groups between pH 7.4 and 5.5 and classified their properties in terms of behaviour under neutral conditions.[16] The spiro-orthoester SpiDo exhibited a hydrolysis half-life $t_{1/2}$ = 1.5 h (assuming a first-order reaction) and complete hydrolysis was obtained after 7 h at pH 5.5.[17] However, to our knowledge, the SpiDo platform has only been used for *in vitro* imaging experiments with microorganelles.

In conclusion, despite the great improvements achieved in pH-sensitive linkers, a new chemistry for versatile linkers with adjustable release rate is still highly desirable for prodrug development, including ADC and gene delivery.

The 1–6 self-immolative elimination process, typical of *p*-amino or *p*-hydroxybenzyl alcohol, is one of the most common processes to drive the release of prodrugs and bioconjugates by external stimuli.[18] We report here a new linker based on the 1–6 self-immolative *p*-hydroxybenzyl alcohol platform designed for the conjugation of a drug to a target system (Scheme 1) and the corresponding release at acid pH. The orthoester group was chosen to provide an effective trigger at pH around 5.5, and the benzyl alcohol moiety was used for binding drugs bearing an amine (as a carbamate) or a phenol (as an aryl benzyl ether). In one side of the aromatic ring, we incorporated a triple bond for click chemistry to bind the cargo to the antibody support. The value of this platform was evaluated in the analysis of cytotoxic drug delivery to cancer cells by conjugation with cetuximab (Ctx), a monoclonal antibody (mAb) specific for epidermal growth factor receptor (EGFR).

Since orthoesters are known to be stable in plasma but sensitive to hydrolysis at pH 5.5,[16,19] we developed an aromatic orthoester derived from gallic acid, a natural tannin component found in several plants and available in large quantities at a low price. Gallic acid (**1**, Scheme 2) already has all the properties for our design: two OH groups to form a cyclic orthoester, another OH for the installation of a triple bond for orthogonal couplings, and the *p*-carboxyl group that can be easily reduced to benzyl alcohol. Thus, gallic acid **1** was esterified to the corresponding ethyl ester **2**, which cyclised with triethyl orthoformate to give the orthoester **3** in high yield (Scheme 2). The remaining free –OH reacted with propargyl bromide **4** (K_2CO_3/KI in dry acetone for 2 h) and the propargyl ether was reduced with $LiAlH_4$ in THF to give the 5-(hydroxymethyl)pyrogallol orthoester derivative **5** (HMPO) in good overall yield starting from **1** (Scheme 2).

Compounds **8** and **11** (Scheme 2) were prepared to evaluate the hydrolysis profile and release of the molecule linked to the benzyloxy group. Activation of **5** with *p*-nitrophenylchloroformate and further reaction with tryptamine **7** in alkaline medium gave carbamate **8** in acceptable yields. After conversion of alcohol **5** to benzyl chloride **9** (see ESI†), nucleophilic displacement with **10** gave phenyl ether **11**. The behaviour of compounds **8** and **11** at different pH values was investigated by HPLC analysis. Compound **8** released the payload almost completely after 7 hours at pH 5.5 (95% release, $t_{(1/2)}$ = 3 h, Fig. S1, ESI†). A comparable kinetics was observed at the same pH with **11** ($t_{1/2} \cong$ 3 h and the 95% of release reached after 6 h, Fig. S2, ESI†). When **8** and **11** were treated at 37 °C at pH 7.4 and 6.5, no significant hydrolysis occurred within 6 h.

Only after 24 h at pH 6.5 the HPLC profile of the samples showed the presence of 10% of tryptamine **7** and 25% of phenol **10** respectively (Fig. S1 and S2, ESI†). These results agreed with those reported for existing orthoester linkers, confirming that HMPO is sensitive to lysosomal pH, showing an excellent stability profile at physiological and extracellular solid tumor pH values.

To get a plausible picture of the disassembling mechanism for HMPO conjugates, we studied the behavior of **11** at pH 5.5 through ^{1}H NMR analysis. The sample was incubated in deuterated acetic buffer at 37 °C and the FID recorded every 30 minutes. After 5 minutes, the shifts of the aromatic signals from δ 7.87 to 7.92 and of the methoxy singlet from δ 4.42 to 4.49 suggested the release of phenol **10** in solution (Fig. S3, ESI†). Moreover, we noticed a new peak at δ 8.69 assigned to the transient assembling of a formate derivative. Finally, the characteristic aromatic and aliphatic signals of a 5-(hydroxymethyl)-3-(2-propynyloxy)pyrogallol (**12**, Scheme 3) were observed, confirming the complete disassembling of the structure and the release of the phenol. An ESI/MS analysis of the solution contained in the NMR tube confirmed the presence of compounds **10** and **12**.

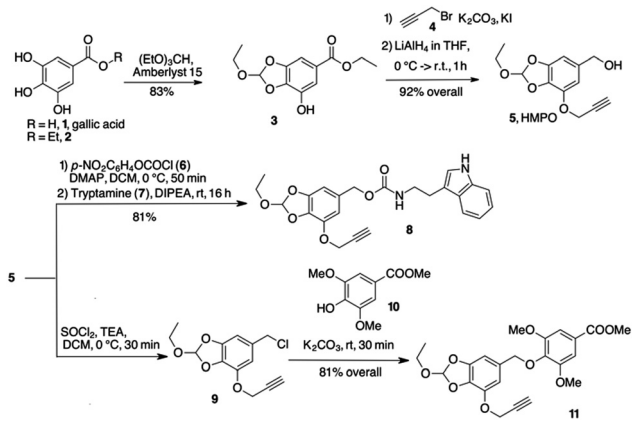

Scheme 2 Synthesis and linkage of HMPO platform.

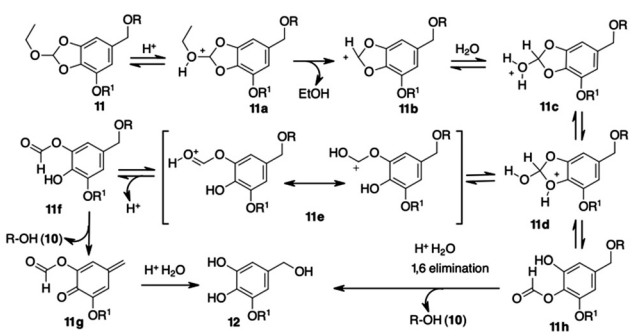

Scheme 3 Proposed mechanism for disassembling of HMPO cargo.

A reasonable mechanism for cargo release from the HMPO platform was then supposed (Scheme 3). In acid conditions, the orthoester moiety is protonated releasing EtOH. The transient (stabilized) carbocation **11b** gives the pyrogallol formate **11f**. The expected 1–6 elimination occurs with formation of *p*-quinone methide **11g** and release of the cargo **10**.

The alternative cleavage of the protonated 2-hydroxybenzodioxole **11d** might give formate **11h** that, after ester hydrolysis, releases the cargo **10** through 1–6 elimination.

We applied the HMPO platform to the conjugation of the antitumor drugs Doxo (**13**) and Combretastatin A4 (**14**) with Cetuximab (Ctx), a monoclonal antibody specific for the epidermal growth factor receptor (EGFR). Activation of **5** with *p*-nitrophenyl chloroformate and further nucleophilic displacement with Doxo gave carbamate **15** in good yield (73%) (Scheme 4). Compound **15** was subjected to CuCAAC reaction with 6-azidohexanoic acid **16** in the presence of Cu(II) acetate and sodium ascorbate in DMF/water, providing compound **17** in 64% yield (Scheme 4). Alternatively, chloride **9** reacted with Combretastatin A4 (**14**), deprotonated by NaH in DMF, to give compound **18** in a good yield (98%). Afterwards, azide **16** gave **19** in 75% yield (Scheme 4).

Molecules **15** and **18** resulted stable in buffers at pH 7.4 and 6.5 (Table S1 and Fig. S4, S5, ESI†). Only a small amount of free Doxo (4%) and Combretastaine A4 (5%) was detected after 24 h at 37 °C at pH 7.4.

The stability in water was investigated to exclude false positive release, confirming that **15** and **18** remain untouched after 24 h at 37 °C in water. A test was also done in human plasma showing a good stability of these compounds (Table 1). The payload **15** showed a $t_{1/2}$ value in line with the general behavior of pure Doxo in plasma.[20] These results confirmed that pH-sensitive HMPO platform is stable to biological fluids as blood. On the other hand, hydrolysis at pH 5.5 showed a rapid release of drugs **13** and **14** (Fig. S4 and S5, ESI†). With **15**, in the first hours a plateau was reached and almost 90% of drug was released after 6 h. Although with a different behaviour, 93% of Combretastatin A4 (**14**) was released from **18** after 12 h (see ESI†).

Table 1 Stability tests of payloads **15** and **18**

Comp.	H_2O[a]	pH 7.4,[a] $t_{1/2}$[b]	pH 6.5,[a] $t_{1/2}$[b]	Plasma,[a] $t_{1/2}$[b]
15	99%	94%, >24 h	90%, >24 h	35%, 8.3 h
18	99%	95%, >24 h	93%, >24 h	89%, 27.6 h

[a] Value expressed as percentage of unmodified compound after 24 h of incubation. [b] Half-life ($t_{1/2}$) expressed as the amount of time it takes before half of the drug is hydrolyzed/degraded.

For the preparation of the ADCs, carboxylic acids **17** and **19** were transformed into the corresponding NHS-esters in PBS at pH 7.4 in presence of Sulfo-NHS (**20**) and EDC, and further reacted with Ctx (Scheme 5) to obtain bioconjugates **21** and **22**. After purification by dialysis, the drug antibody ratio (DAR) was determined by MALDI analysis (Table S1, ESI†). A HPLC/MS analysis of the dialyzed solution showed the absence of the free drugs **13** and **14** in solution. The anti-proliferative activity (MTT assay) of the conjugate **21** and **22** was evaluated in A549 (human lung carcinoma, Fig. 1) and A431 (epidermoid carcinoma cell line, Fig. S7, ESI†), both overexpressing the epidermal growth factor receptor (EGFR). Treatment with the two conjugates showed a stronger antiproliferative effect if compared with unconjugated Ctx (Fig. 1). The effect was also comparable to the activity of the free drugs confirming the release of Doxo and Combretastatin A4 from the linker in the cell culture. The observed differences between the release kinetics of **15** and **18** and the cell viability assays of the corresponding conjugates **21** and **22** might be due to the different mechanism of action of the two drugs (intercalation into DNA and inhibition of topoisomerase II for Doxo *versus* depolymerisation of tubulin for Combretastatin A4), which probably requires different times of action.

HMPO alone wasn't toxic, on the other hand, on cells employed in the tests. DAPI staining, Annexin V-FITC and PI staining tests were also employed to investigate the pathway of cell death. The results showed that **21** and **22** significantly induce apoptosis and cell death (Fig. S7 and S8, ESI†).

In conclusion, we demonstrated that the new HMPO platform (**5**) can be employed for drug delivery in acid biologic

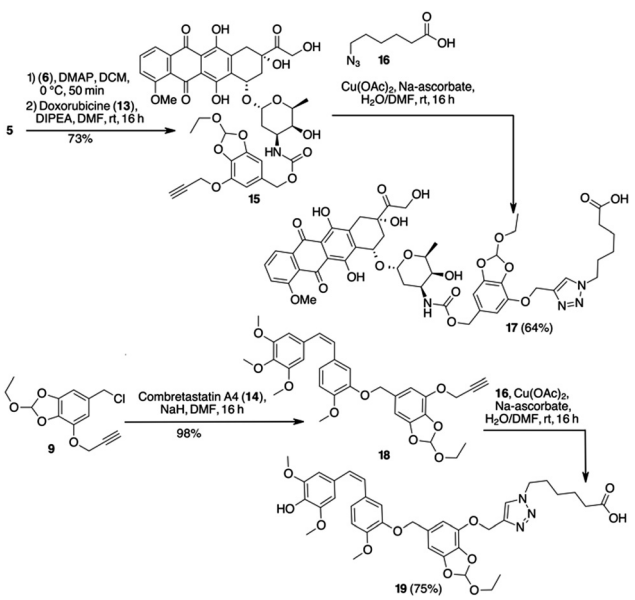

Scheme 4 Conjugation of Doxo and Combretastatin A4 with HMPO.

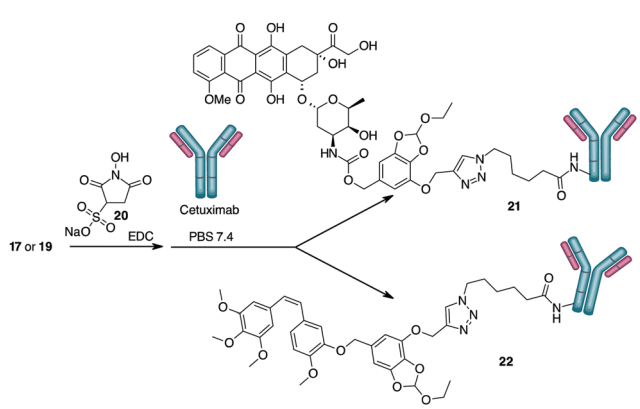

Scheme 5 ADC preparation.

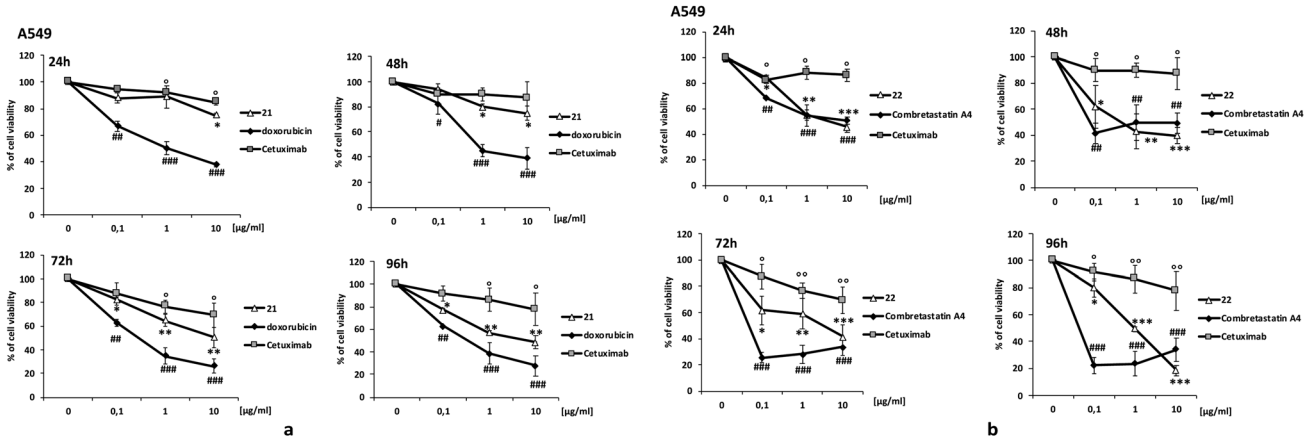

Fig. 1 Cell viability. Cancer cell survival was evaluated by MTT test. Cells were exposed to increasing concentration of: (a) conjugate **21**, Doxorubicin and Cetuximab; (b) conjugate **22**, Combretastatin A4 and Cetuximab. Data are expressed as percent of cell viability. $^{\#}$,*, $^{\circ}$ $p < 0.05$ *vs.* basal; $^{\#\#}$,**, $^{\circ\circ}$ $p < 0.01$ *vs.* basal and $^{\#\#\#}$,***, $^{\circ\circ\circ}$ $p < 0.001$ *vs.* basal.

environments resulting suitable for conjugation of the cytotoxic drugs Doxo (a primary amine) and Combretastatin A4 (a phenol) with an antibody carrier. The resulting ADCs exhibited improved cytotoxic activity in cancer cells compared to the unconjugated antibody and to the cargo-linker fragment.

Various primary and secondary amine-, alcohol- and phenol-containing molecules can be bound by the formation of carbamates, carbonates or ethers. Orthogonal reactivity to these bonds is possible by introducing azides, alkynes, tetrazines or other fragments for click chemistry to allow easy conjugation with macromolecular supports. HMPO has the same stability and other typical properties as other pH-reactive linkers, but is non-toxic and easily accessible synthetically (4 steps, 76% overall yield) from gallic acid, a cheap natural starting material. Ultimately, the low toxicity suggests a potential use of our linker in non-oncology therapies. Application of the linker to non-canonical cytotoxic drugs for intra- and extracellular delivery is in preparation and will be reported shortly.

This work was supported by the AIRC (under IG 2017 – ID. 20758 project – P. I. Taddei Maurizio).

Conflicts of interest

There are no conflicts to declare.

Notes and references

1 X. Yang, Z. Pan, M. R. Choudhury, Z. Yuan, A. Anifowose, B. Yu, W. Wang and B. Wang, *Med. Res. Rev.*, 2020, **40**, 2682–2713.
2 (*a*) K. C. Nicolaou and S. Rigol, *Angew. Chem., Int. Ed.*, 2019, **58**, 11206–11241; (*b*) K. Tsuchikama and Z. An, *Protein Cell*, 2018, **9**, 33–46; (*c*) V. Chudasama, A. Maruani and S. Caddick, *Nat. Chem.*, 2016, **8**, 114–119.
3 (*a*) L. Battistini, K. Bugatti, A. Sartori, C. Curti and F. Zanardi, *Eur. J. Org. Chem.*, 2021, 2506–2528; (*b*) B. Alday-Parejo, R. Stupp and C. Rüegg, *Cancers*, 2019, **11**, 978; (*c*) P. Zhong, X. Gu, R. Cheng, C. Deng, F. Meng and Z. Zhong, *Int. J. Nanomed.*, 2017, **12**, 7913–7921; (*d*) D. Arosio and C. Casagrande, *Adv. Drug Delivery Rev.*, 2016, **97**, 111–143; (*e*) J. S. Desgrosellier and D. A. Cheresh, *Nat. Rev. Cancer*, 2010, **10**, 9–22.
4 (*a*) A. Janoniene and V. Petrikaite, *Mol. Pharm.*, 2020, **17**, 1800–1815; (*b*) S. Cazzamalli, A. Dal Corso, F. Widmayer and D. Neri, *J. Am. Chem. Soc.*, 2018, **140**, 1617–1621.
5 (*a*) A. Rana and S. Bhatnagar, *Bioorg. Chem.*, 2021, **112**, 104946; (*b*) M. Scaranti, E. Cojocaru, S. Banerjee and U. Banerji, *Nat. Rev. Clin. Oncol.*, 2020, **17**, 349–359; (*c*) J. A. Reddy, R. Dorton, A. Bloomfield, M. Nelson, C. Dircksen, M. Vetzel, P. Kleindl, H. Santhapuram, I. R. Vlahov and C. P. Leamon, *Sci. Rep.*, 2018, **8**, 8910–8943; (*d*) Y. Cao and J. Yang, *Bioconjugate Chem.*, 2014, **25**, 873–878.
6 X. Wang, A. Shirke, E. Walker, R. Sun, G. Ramamurthy, J. Wang, L. Shan, J. Mangadlao, Z. Dong, J. Li, Z. Wang, M. Schluchter, D. Luo, Y. Wang, S. Stauffer, S. Brady-Kalnay, C. Hoimes, Z. Lee and J. P. Basilion, *Cancers*, 2021, **13**, 417.
7 (*a*) A. Dal Corso, *ChemBioChem*, 2020, **21**, 3321–3322; (*b*) A. Dal Corso, L. Pignataro, L. Belvisi and C. Gennari, *Chem. – Eur. J.*, 2019, **25**, 14740–14757; (*c*) T. Chatzisideri, G. Leonidis and V. Sarli, *Future Med. Chem.*, 2018, **10**, 2201–2226; (*d*) M. Huo, Q. Zhu, Q. Wu, T. Yin, L. Wang, L. Yin and J. Zhou, *J. Pharm. Sci.*, 2015, **104**, 2018–2028.
8 A. Alouane, R. Labruére, T. Le Saux, F. Schmidt and L. Jullien, *Angew. Chem., Int. Ed.*, 2015, **54**, 7492–7509.
9 (*a*) A. Beck, L. Goetsch, C. Dumontet and N. Corvaïa, *Nat. Rev. Drug Discovery*, 2017, **16**, 315–337; (*b*) R. V. J. Chari, M. L. Miller and W. C. Widdison, *Angew. Chem., Int. Ed.*, 2014, **53**, 3796–3827.
10 V. Estrella, T. Chen, M. Lloyd, J. Wojtkowiak, H. H. Cornnell, A. Ibrahim-Hashim, K. Bailey, Y. Balagurunathan, J. M. Rothberg, B. F. Sloane, J. Johnson, R. A. Gatenby and R. J. Gillies, *Cancer Res.*, 2013, **73**, 1524–1535.
11 H. T. McMahon and E. Boucrot, *Nat. Rev. Mol. Cell Biol.*, 2011, **12**, 517–533.
12 (*a*) S. Chu, X. Shi, Y. Tian and F. Gao, *Front. Oncol.*, 2022, 12; (*b*) R. Gannimani, P. Walvekar, V. R. Naidu, T. M. Aminabhavi and T. Govender, *J. Controlled Release*, 2020, **328**, 736–761.
13 J. D. Bargh, A. Isidro-Llobet, J. S. Parker and D. R. Spring, *Chem. Soc. Rev.*, 2019, **48**, 4361–4374.
14 A. Luong, T. Issarapanichkit, S. D. Kong, R. Fong and J. Yang, *Org. Biomol. Chem.*, 2010, **8**, 5105–5109.
15 (*a*) A. Zhang, L. Yao and M. An, *Chem. Commun.*, 2017, **53**, 12826–12829; (*b*) S. Su, F. S. Du and Z. C. Li, *Org. Biomol. Chem.*, 2017, **15**, 8384–8392.
16 S. A. Jacques, G. Leriche, M. Mosser, M. Nothisen, C. D. Muller, J.-S. Remy, A. Wagner, J. Delahousse, C. Skarbek and A. Paci, *Org. Biomol. Chem.*, 2016, **14**, 4794–4803.
17 G. Leriche, M. Nothisen, N. Baumlin, C. D. Muller, D. Bagnard, J.-S. Remy, S. A. Jacques and A. Wagner, *Bioconjugate Chem.*, 2015, **26**, 1461–1465.
18 A. Abe and M. Kamiya, *Bioorg. Med. Chem.*, 2021, **44**, 116281.
19 Z. Khademi and K. Nikoofar, *RSC Adv.*, 2020, **10**, 30314–30397.
20 N. Laubrock, G. Hempel, P. Schulze-Westhoff, G. Würthwein, S. Flege and J. Boos, *Chromatographia*, 2000, **52**, 9–13.